TRAIN in response to treatment with anti-cancer small molecule destabilizing chromatin

Katerina Leonova[1], Alfiya Safina[1], Elimelech Nesher[1,2], Poorva Sandlesh[1], Rachel Pratt[1], Catherine Burkhart[3], Britney Lipchick[1], Costakis Frangou[1], Igor Koman[2], Jianmin Wang[4], Kirill Kirsanov[5], Marianna G. Yakubovskaya[5], Andrei V. Gudkov[1], Katerina Gurova[1,#]

1 – Department of Cell Stress Biology, Roswell Park Cancer Institute, Buffalo, NY, 14263, USA

2 – Department of Molecular Biology, Ariel University, Ariel 40700, Israel

3 – Buffalo BioLabs, 71 High Str, Buffalo, NY 14263, USA

4 - Department of Bioinformatics, Roswell Park Cancer Institute, Buffalo, NY, 14263, USA

5 - Department of Chemical Carcinogenesis, Institute of Carcinogenesis, Blokhin Cancer Research Center RAMS, Moscow 115478, Russia

[#]**Corresponding author:** Katerina Gurova, Department of Cell Stress Biology, Roswell Park Cancer Institute, Elm and Carlton Streets, Buffalo, NY 14127, USA; Tel# 1-716-845-4760, Fax# 1-716-845-3944, e-mail: katerina.gurova@roswellpark.org

Funding

This work was supported by Incuron LLC to K.G.; by National Cancer Institute [R01CA197967 to K.G. and P30CA016056 to Roswell Park Cancer Center.

Abstract

Genome stability is in the focus of research for many decades, while stability and integrity of chromatin is far less studied. Cell identity in multicellular organism is completely dependent on chromatin stability, therefore there should be mechanisms ensuring maintenance of epigenetic integrity. Previously, we have found that loss of DNA methylation in the absence of p53 leads to the transcription of silenced repetitive elements, such as pericentromeric repeats and endogenous viruses, what causes activation of IFN response, similarly to viral invasion, and IFN-dependent cell death. We named this phenomenon TRAIN (**T**ranscription of **R**epeats **A**ctivates **IN**terferon). Now we found that small molecule, curaxin, which destabilizes nucleosome via binding to DNA and deforming helix shape, causes TRAIN independently on p53 status. Curaxin demonstrated activity as cancer treatment and preventive agent via established previously p53 activating and NF-kappaB inhibiting activities. Here we showed that activation of IFN response is an additional mechanism of inhibition of oncogene-induced transformation by curaxin. Our data suggest that TRAIN is a response to the loss of chromatin stability and one of the mechanisms which prevents oncogene-induced transformation.

Introduction

There are multiple mechanisms to control proper storage of genetic information, including response to different sorts of DNA damage, negative selection against cells with impaired DNA and several specialized DNA repair pathways (reviewed in (Miller, 2010, Wang & Lindahl, 2016)). Not less important, epigenetic, information is stored in the form of chromatin, highly-organized complex of DNA, histone and non-histone proteins and their chemical modifications (reviewed in (Campos, Stafford et al., 2014, Miska & Ferguson-Smith, 2016)). Destabilization of chromatin should lead to the dysregulation of cellular transcriptional program and loss of cell identity, which is crucial for multicellular organism. One of the examples demonstrating high stability of cellular epigenome is well known extremely low efficiency of reprogramming of differentiated cell (reviewed (Ebrahimi, 2015, Hussein & Nagy, 2012)). Another one is an absence of one common "cancer cell" phenotype: all tumors, including cell lines, propagated for years in culture, bear easily identifiable traits of tissue of origin in their transcriptional program. Nonetheless, we do not know what mechanisms control stability of chromatin in cells, i.e. whether there is any sort of stress response to chromatin destabilization, as well as negative selection against cells which lose epigenetic integrity.

One of the reasons of this deficit was absence of tools to induce chromatin "damage" without simultaneous introduction of DNA damage. This possibility appeared, when we found anti-cancer small molecules, known as curaxins cause chromatin disassembly in cells in the absence of DNA damage (Gasparian, Burkhart et al., 2011), (Safina, Cheney et al., 2017). They were identified in a phenotype based screening for the ability to activate p53 and inhibit NF-kappaB simultaneously (Gasparian et al., 2011). Search for the mechanism of action of curaxins led us to the finding that they bind DNA via intercalation of carbazole body accompanied with protrusion of two side chains into major groove and third side chain into minor groove of DNA. Curaxins have no effect on DNA chemical structure, i.e. they do not cause any sort of DNA damage in mammalian cells, however, their binding to DNA does change DNA helical shape, flexibility, as well as reduce negative charge of DNA (Safina et al., 2017).

Structural unit of chromatin in eukaryotic cells is nucleosome, consisting of a core of positively charged histone proteins, wrapped in negatively charged DNA. Stability to the nucleosome is based on the electrostatic interactions between histones and phosphate backbone of DNA supported by several precisely spatially oriented points of contact between histone amino acids and base pairs of DNA (Luger, Mader et al., 1997). When nucleosomal DNA is unwrapped due to any reason, core becomes unstable due to repulsion of positively charged histones from each other. Alterations of DNA helical shape, charge and flexibility, caused by curaxins, force DNA to dissociate from the core *in vitro* and *in vivo* (Safina et al., 2017). At lower concentrations of curaxin, CBL0137, DNA is first unfolded from outer parts of nucleosome, i.e. from H2A/H2B dimers located at both sides of inner H3/H4 tetramer. This leads to the detachment of H2A/H2B dimers(s) and exposure of the surface of H3/H4 tetramer. At higher concentrations of CBL0137, DNA is unwrapped from inner H3/H4 tetramer leading to the complete nucleosome disassembly (Safina et al., 2017). At the regions where DNA helix loses histone cores it becomes significantly under twisted, which in principle may be alleviated via activity of topoisomerases or free rotation of DNA. However, in cells free rotation is almost impossible due to the length of DNA and binding to multiple proteins. Moreover, topoisomerases cannot cleave DNA in the presence of curaxins (Safina et al., 2017). In these conditions excessive energy of negative supercoiling causes base unpairing and DNA transition from B-DNA into alternative non-B DNA structures. We have shown massive transition of right-handed B-DNA in CBL0137 treated cells into left-handed Z-DNA form (Safina et al., 2017). Thus, treatment of cells with CBL0137 leads to dose-dependent destabilization and disassembly of chromatin in the absence of DNA damage and, most importantly, of classical DNA damage

response, providing an opportunity to study how cell reacts to chromatin damage as well as the role of chromatin perturbations in anti-cancer activity of curaxins.

First type of response which we observed in curaxin treated cells was activation of p53, well-known reaction of cells to DNA damage. However, no phosphorylation of p53 N-terminal serines, obligatory marks of DNA damage response, was detected in curaxin treated cells, as well as no activation of DNA-damage sensitive kinases, such as ATM, ATR, DNA-PK etc. p53 in curaxin treated cells was phosphorylated at serine 392 by casein kinase 2 being in a complex with histone chaperone FACT (Gasparian et al., 2011). FACT consists of two conservative proteins present in all eukaryotes, Suppressor of Ty 16 (SPT16) and Structure Specific Recognition Protein 1 (SSRP1). In basal conditions, FACT binds histone oligomers via different domains of SSRP1 and SPT16, weakening their contact with DNA and making the latter available for transcription (Valieva, Armeev et al., 2016, Winkler & Luger, 2011). FACT binding prevents histone oligomers from dissociation, while DNA is transcribed (Belotserkovskaya, Oh et al., 2003). We have found that nucleosome disassembly caused by curaxin, opens multiple sites for FACT binding normally shielded inside nucleosome. Chromatin unfolding occurs first in heterochromatic regions and all cellular FACT are rapidly relocated into these regions and depleted from nucleoplasm (Safina et al., 2017). We named this phenomenon chromatin-trapping or c-trapping. Although curaxins do not bind and inhibit FACT directly, they cause exhaustion of FACT and trapping it in heterochromatin, therefore c-trapping is equivalent of functional FACT inhibition. We also observed that FACT not only binds partially disassembled nucleosome, but FACT also Z-DNA via CID (c-terminal intrinsically disordered) domain (Safina et al., 2017). Importantly, it was already known that the immediate neighboring domain, HMG (high mobility group), also bind non-B DNA, bent or cruciform (Gariglio, Ying et al., 1997, Krohn, Stemmer et al., 2003, Yarnell, Oh et al., 2001). In all cases of SSRP1 binding to DNA there is CK2-mediated signal for p53 activation (Gasparian et al., 2011, Krohn et al., 2003). Therefor c-trapping may be a part of general response to the destabilization of chromatin and may serve for recruitment of FACT to the regions of potential nucleosome loss to prevent this loss and to restore chromatin structure.

However, there are many unclear issues within this model. Among the most immediate are two related questions: (i) what are the consequences, besides c-trapping, of nucleosome destabilization and chromatin unfolding in cells? (ii) Whether all effects of curaxins may be explained by functional inactivation of FACT. In this study, we tried to answer these questions starting from the comparison of the effects of CBL0137 on transcription. We found, that independently on the presence of FACT, CBL0137 activates transcription from heterochromatic regions normally silenced in cells, including centromeric and pericentromeric repeats and endogenous retroviral elements resulting in accumulation of double stranded RNAs (dsRNA) in cells and activation of interferon (IFN) response. This phenomenon, named TRAIN (Transcription of Repeats Activates INterferon) (Leonova, Brodsky et al., 2013) was observed before upon DNA demethylation (Chiappinelli, Strissel et al., 2015, Guryanova, Shank et al., 2016, Roulois, Loo Yau et al., 2015). Although, IFN activation has been traditionally viewed as a part of antiviral defense, TRAIN may present a more general cell response to the problems associated with chromatin organization in cells or a defense against loss of epigenetic integrity. We proposed that the reason of TRAIN in CBL0137 treated cells is direct effect of the drug on nucleosome structure leading to the opening of chromatin.

Material and Methods

Chemical, Reagents and Plasmids*:* CBL0137 was provided by Incurone, LLC. Trichostatin A was purchased from Sigma-Aldrich. Poly I:C (polyinosinic:polycytidylic acid) was purchased

from Tocris Bioscience. ISRE-mCherry reporter plasmid was purchased from Cellecta. Two ZBP1 gRNA, control gRNA and CRISPR/Cas9 lentiviral single vector plasmids and mCherry-tagged histone H1.5 were purchased from GeneCopoeia. GFP-tagged SSRP1 was already described in (Safina et al., 2017).

Cells: HeLa, HepG2 and HT1080 cells were from ATCC, they were maintained in DMEM with 5% Fetal Bovine Serum and 50ug/ml of penicillin/streptomycin. Mouse squamous cell carcinoma SCCVII cells were obtained from Dr. Burdelya (Roswell Park Cancer Institute, Buffalo, NY). Preparation and maintenance of HeLa-TI cell populations containing integrated avian sarcoma genome with silent green fluorescent protein (GFP) gene were described previously (Poleshko, Einarson et al., 2010, Shalginskikh, Poleshko et al., 2013).

Isolation and cultivation of mouse embryonic fibroblast (MEF) cells: MEFs were isolated from 13.5-days post-coitus embryos by breeding C57BL/6 mice p53-heterozygous ($p53^{+/-}$) and from C57BL/6 IFNAR-null and p53-heterozygous females and males as described in the protocol http://www.molgen.mpg.de/~rodent/MEF_protocol.pdf. Cells from each embryo were individually plated. DNA was isolated from individual embryos by PureLink^{TM} Genomic DNA Kit (Invitrogen). The genotype of the embryos was determined by PCR with the following primers: $p53^{+/+}$ ACAGCGTGGTGGTACCTTAT; $p53^{+/-}$ TATACTCAGAGCCGGCCT; $p53^{-/-}$ TCCTCGTGCTTTACGGTATC; IFNARko 5'common 5'-ATTATTAAAAGAAAAGACGAGGAGGCGAAGTGG-3'; IFNARko 3'WTallele 5'-AAGATGTGCTGTTCCCTTCCTCTGCTCTGA-3'; IFNARko Neo 5'-CCTGCGTGCAATCCATCTTG-3'. MEF cells were cultured in DMEM supplemented with 10% FBS and 50ug/ml of penicillin/streptomycin for no more than 8 passages.

Reverse transcriptase-PCR: cDNA was made from 1µg of total RNA isolated by TRIzol (Invitrogen) by using iScript cDNA Synthesis Kit (BioRad). The PCR reaction was carried out in accordance with manufacturing protocol of Taq PCR Master Mix (USB) in a reaction volume of 25µl with 100ng of the following primers: mouse Irf7 (sense: 5'-CAGCCAGCTCTCACCGAGCG; antisense: 5'-GCCGAGACTGCTGCTGTCCA), mouse Ifit3 (Isg49) (sense: 5'-GCCGTTACAGGGAAATACTGG; antisense: 5'-CCTCAACATCGGGGCTCT); human ISG56 (sense: 5'- CCCTGCAGAACGGCTGCCTA; antisense: 5'-AGCAGGCCTTGGCCCGTTCA); mouse Isg15 (sense: 5'-AAGAAGCAGATTGCCCAGAA; antisense: 5'-TCTGCGTCAGAAAGACCTCA); mouse Usp18 (sense: 5'-AAGGACCAGATCACGGACAC; antisense: 5'- CACATGTCGGAGCTTGCTAA), mouse-β-actin (sense: 5'-GCTCCGGCATGTGCAA; antisense: 5'-AGGATCTTCATGAGGTAGT-3'), human ZBP1 (sense: 5'- TGCAGCTACAATTCCAGAGA; antisense: 5'- GAAGGTGCCTGCTCTTCATC.

Western immunoblotting: Protein extracts were prepared by lysing cells or tissues in RIPA buffer (Sigma-Aldrich) with protease inhibitor cocktail (Sigma-Aldrich). Extracts were spun down at 10,000xrpm for 10minutes at 4^{o}C to obtain the soluble fraction. Protein concentrations were determined by BioRad Protein Asssay (Bio-Rad). Equal amounts of protein were run on gradient 4-20% precast gels (Invitrogen) and blotted/transferred to Immobilon-P membrane (Millipore). Membranes were blocked with 5% non-fat milk-TBS-T buffer for 1 hour and incubated overnight with primary antibodies. The following antibodies were used: 1:10000 anti-ISG49 and anti-ISG56 (a kind gift of Dr. Ganes Sen, Cleveland Clinic). To verify equal protein loading and transfer β-actin (Santa Cruz) antibodies were used. Anti-mouse and anti-rabbit secondary horseradish peroxidase-conjugated antibodies were purchased from Santa Cruz. ECL detection reagent (GE Healthcare) was used from protein visualization onto Autoradiography film (Denville Scientific).

Northern hybridization: Mouse cDNA probes for SINE B1 (sense: 5'-GCCTTTAATCCCAGCACTTG, antisense: 5'-CTCTGTGTAGCCCTGGTCGT), were made by reverse-PCR from total RNA of MEF cells. The cDNAs were labeled with [α^{32}P]dCTP, using the Random Primed DNA Labeling Kit following the protocol provided by Roche (Mannheim, Germany).

Total RNA was extracted from cells that were either untreated or treated with 10μM of 5-aza-dC for 48 hours or 0.5uM of CBL0137 for 24 hours using Trizol (Invitrogen). A measure of 5 μg of total RNA was loaded onto each lane, electrophoresed in an agarose–formaldehyde gel and transferred onto a Hybond-N membrane (Amersham Pharmacia Biotech). After UV crosslinking, the transfers were hybridized with [α^{32}P]dCTP-labeled probes and analyzed by autoradiography at -80°C.

Immunofluorescent staining: Cells were plated in 35mm glass bottom plates from MatTek Corporation (Ashland, MA). After treatments cells were washed with PBS and fixed in 4% paraformaldehyde at room temperature for 15 min. For Z-DNA staining, a 4% paraformaldehyde solution containing 0.1% Triton-X100 in PBS was added to cells for 15 min immediately after removal of media. Cells were then washed 3 times with PBS. Blocking was done in 3% BSA, 0.1% Triton-X100 in PBS. Primary antibodies, Z-DNA from Abcam (cat# ab2079) was used at 1:200 dilution. dsRNA antibody (J2) from Scicons (Hungary) was used at 1:50 dilution. AlexaFluor 488 or 594 donkey anti-mouse (Invitrogen, cat# A21206; 1:1000) and AlexaFluor 594 donkey anti-sheep (Jackson ImmunoResearch, cat# 713-585-147; 1:500) were used as a secondary antibodies. Antibodies were diluted in 0.5% BSA + 0.05% Triton X100 in PBS. After each antibody incubation, cells were washed three times with 0.05% Triton X100 in PBS. For DNA counterstaining, 1μg/ml solution of Hoechst 33342 in PBS was used. Images were obtained with a Zeiss Axio Observer A1 inverted microscope with N-Achroplan 100×/1.25 oil lens, Zeiss MRC5 camera, and AxioVision Rel.4.8 software.

Flow cytometry was performed on LSR Fortessa A and BD LSRII UV A Cytometers (BD Biosciences, San Jose, CA, USA). Obtained data were analyzed by WinList 3D program (Verity Software House, Topsham, ME, USA).

Microarray hybridization, RNA-sequencing and analyses: Total RNA from cells was isolated using Trizol reagent (Invitrogen). Three biological replicates of each condition were used for microarray hybridization and two – for RNA-sequencing. RNA processing, labeling, hybridization, libraries generation and sequencing were done in RPCI Genomics facility. MouseWG-6 v2.0 Expression BeadChip array (Illumina) was used for hybridization. TruSeq Stranded Total RNA Library Prep Kit with Ribo-Zero Mouse kit (Illumina) was used for library preparation. Sequencing was done using Illumina HiSeq 2000 system. Gene expression data were analyzed using GeneSpring GX for microarray hybridization and Strand NGS for RNA-sequqncing (Agilent Genomics, Santa Clara, CA, USA). GSEA was done using MSigDB (Broad Institute) and MetaCore software (Thompson Reuter).

The GRCm38.p5 (Genome Reference Consortium Mouse Reference 38) assembly was used for all mouse data, and the set of annotated repeat types was taken from the Repbase database (Kapitonov & Jurka, 2008). Sailfish version 0.6.3 aligner was used to quantify the abundance of previously annotated RNA transcripts from RNA-seq data (Patro, Mount et al., 2014). Analyses were performed with a modified k-mer size of k = 17 and used 16 concurrent threads (p 16). Sailfish was run with the polya option, which discards k-mers consisting of k consecutive A's or T's, and bias correction was enabled. Importantly, a read was associated with a particular

'repeat' type if it satisfied the following criteria: a), the read aligned to a single or multiple locations within the canonical sequence of that repeat type, or annotated instances of that repeat type within the genome, incorporating 13 bp (half of read length) genomic sequences flanking the annotated instances; b), no alignment of such or better quality to canonical or instance sequences associated with any other annotated repeat types could be obtained. An optional masking procedure, designed to exclude reads potentially originating from un-annotated repeat types, added a third requirement: c), no alignment of such or better quality to any portion of the genome assembly that is not associated with the annotated instances of that repeat type could be obtained. Collectively, the combined repeat assembly file contained a single FASTA entry for each repeat type as defined in the Repbase database. The Transcripts per Million quantification number was computed as described in (Wagner, Kin et al., 2013), (Qian & Huang, 2005) and is meant as an estimate of the number of transcripts, per million observed transcripts, originating from each target transcript. Its benefit over the F/RPKM measure is that it is independent of the mean expressed transcript length (i.e. if the mean expressed transcript length varies between samples, for example, this alone can affect differential analysis based on the K/RPKM). Finally, we used the variational Bayesian EM algorithm integrated in sailfish, rather than the “standard” EM algorithm to optimize abundance estimates. P values were corrected using an FDR correction using the method.

Statistical analyses: Unpaired t-test was used for comparison of quantitative data between control and experimental groups. Analyses were conducted using SAS v9.4 (Cary, NC) and all p-values are two-sided.

Animal experiments: All experiments were reviewed and approved by RPCI IACUC. Mice were maintained in the Department of Laboratory Animals with controlled air, light and temperature conditions, fed ad libitum and free access to water. NIH Swiss and C57Bl/6J mice were purchased from Jackson Lab.

For the analysis of gene expression groups of three mice, female 6-8 weeks old, were treated with one dose of CBL0137 dissolved in 5% dextrose intravenously via tail vein, control mice received injection of 5% dextrose.

For the comparison of efficacy of different doses of CBL0137 SCID male mice 6-8 weeks old were inoculated with 10(6) of HepG2 cells in PBS into two flanks. When tumors reach ~50mm3, mice were randomized into 4 groups of 5 mice. Treatment was done once a week intravenously.

Results

Treatment with CBL0137 changes transcription of genes in FACT positive and negative tissues

The effect of CBL0137 on gene expression may be due to its binding to DNA and the unfolding of chromatin or due to the functional inhibition of FACT. To detect the potential FACT-independent effects of CBL0137, we sought to compare gene expression profiles in FACT-positive and negative cells before and after CBL0137 treatment. All tumor and non-tumor cell lines tested to date express FACT subunits at different levels. The suppression of FACT expression with shRNA resulted in either partial reduction of FACT expression or complete knockdown of FACT in only a fraction of cells, which are quickly overgrown by FACT-positive

cells (Carter, Murray et al., 2015, Dermawan, Hitomi et al., 2016, Safina, Garcia et al., 2013). To overcome this problem, we tested the effect of CBL0137 *in vivo* in tissues that either naturally express FACT or not. Liver and lung were selected as FACT-negative, and spleen and testis were used as FACT-positive tissues ((Garcia, Fleyshman et al., 2011) and Fig. 1A). Gene expression in these tissues was compared in mice treated with different doses of CBL0137 24 hours prior to organ collection. The three doses used represented different degrees of anti-cancer activity (weak, intermediate, and strong) with 90 mg/kg being close to the maximal tolerable dose (Fig.S1A).

Hybridization analysis using mouse Illumina BeadChip array showed that all samples were clustered according to their tissue of origin and dose of CBL0137 (Fig.S1B). The liver and spleen samples from the vehicle- or 30mg/kg of CBL0137-treated mice were grouped together, suggesting little or no effect of this dose on gene expression in the tested organs (Fig.S1B). Samples from mice treated with 60 and 90 mg/kg CBL0137 were also grouped together (spleen, testis) or close to each other (liver, lung), demonstrating a minimal difference between these doses. Surprisingly, very few genes changed expression in the testis (FACT positive organ (Fig.S1C), which may be due to either limited accumulation of the drug in testis due to blood-testis barrier ("Sertoli cell barrier" (Mruk & Cheng, 2015) or the specific chromatin structure in this organ (Wu & Chu, 2008). Maximal changes were observed in the FACT-positive spleen followed by lung and liver (FACT-negative organs) (Fig.S1C). The changes in gene expression caused by CBL0137 in these FACT-negative tissues suggest a FACT independent mechanism.

There was almost no overlap in genes down-regulated in response to CBL0137 among different organs (Fig. 1B), however, one gene, Ifit3, was upregulated in all organs (Fig.1C, D). Many transcripts in two or three organs increased similarly in a dose-dependent manner in response to CBL0137 (Fig.1C, D), suggesting that there may be a common pathway(s) induced by CBL0137 independently of FACT. To identify this pathway(s) we performed gene set enrichment analysis (GSEA) using the Molecular Signature Data Base (Broad Institute). The pathway that was upregulated in response to doses above 30mg/kg in all organs with the exception of testis, which was not analyzed due to the low number of upregulated genes, was interferon (IFN) signaling (Fig.2A and Supplemental Tables S1-6). The same pathway was ranked first when the list of genes that were upregulated in response to CBL0137 in two or more organs was analyzed (Fig.2B). Transcription factors, which regulate genes that were elevated in response to CBL0137, are Stat1, Irf1, Irf8 and Irf7 (Fig.2C). Part of the upregulated genes were targets of Sp1 in lung and p53 in the spleen (Fig.S3). This analysis suggested that CBL0137 treatment leads to the activation of the IFN response in all tissues independently of FACT expression, while p53 was activated only in the FACT positive spleen as it was expected (Gasparian et al., 2011).

CBL0137 treatment causes rapid and robust IFN response in mouse tissues

We have shown previously that CBL0137 inhibits NF-kappaB via a FACT-dependent mechanism (Gasparian et al., 2011), therefore the activation of IFN response was an unexpected finding, because the two pathways, NF-kappaB and IFN, have multiple common inducers and regulators (reviewed in (Pfeffer, 2011)). Hence, we confirmed the microarray data using different approaches. We observed an increase in the liver, lung and spleen of the mRNA level of Irf7, a transcriptional factor whose expression is induced by IFN (Wathelet, Lin et al., 1998), following treatment with greater than 30 mg/kg CBL0137 (Fig.3A and S4A). The same trend was observed in testis, but it did not reach statistical significance. Activation of the IFN

response was confirmed using a second mouse strain by RT-PCR detection of an expanded set of IFN-inducible mRNAs, and at the protein level in spleen using an antibody to ISG49, the protein encoded by Ifit3 gene (Fig.3B, C and S4B).

There are multiple known inducers of the IFN response, among which are components of viruses (e.g. dsRNA, cytoplasmic DNA), cytokines, DNA damage, demethylation of genomic DNA, etc (reviewed in (Silin, Lyubomska et al., 2009)). Based on the literature, the kinetics of the IFN response is different depending on the inducer, with viral components and cytokines being the quickest (minutes – several hours (Silin et al., 2009), followed by DNA damage (16-48 hours (Brzostek-Racine, Gordon et al., 2011) and demethylating agents (>48 hours (Leonova et al., 2013)). To compare the effect of CBL0137 vis-à-vis these stimuli, we assessed the kinetics of induction of the IFN response after CBL0137 treatment. We first measured Irf7 mRNA in the spleen and lung of mice treated with 3 doses of CBL0137 for 24, 48, or 96 hours prior to organ collection. The peak of induction was already seen at 24 hours following treatment with either 60 or 90 mg/kg CBL0137, while 30 mg/kg showed slower kinetics (Fig. 3D, E and Fig.S5A, B). Increased levels of two other IFN responsive genes, Isg15 and Usp18, were detected as early as 6 hours post-treatment with 90 mg/kg dose of CBL0137, and reached a peak at 12 hours, which then gradually declined (Fig.3F, G and Fig.S5C). Similar kinetics was observed at the protein level (Fig.3H). Thus, the CBL0137-induced IFN response is faster than that reported with other small molecules, and is closer to the response observed with biologicals.

Increased expression of IFN responsive genes induced by CBL0137 is dependent on IFN signaling

Experiments with mice demonstrated that CBL0137 caused a rapid and robust induction of the IFN response in all tissues of mice that were tested. To investigate the mechanism of this phenomenon, we modeled this effect *in vitro* using normal and tumor cells (mouse and human). We detected an increase in mRNA and protein levels of IFN-inducible genes in both human and mouse fibroblasts (Fig.4A-C), but not in tumor cells of mouse or human origin (data not shown). Since different components of the IFN response are frequently inactivated in tumors (Kulaeva, Draghici et al., 2003), we employed a reporter assay that detected an IFN response through the activation of a consensus IFN-sensitive response element (ISRE) that drove the expression of mCherry (Imam, Ackrill et al., 1990). Polyinosinic-polycytidylic acid (poly(I:C)), a synthetic analog of double-stranded RNA (dsRNA), was used as a positive control for reporter activity. Using this assay, we observed that CBL0137 induces IFN response also in tumor cells, mouse and human (Fig.4 D, E).

The next step towards the mechanism of CBL0137-activated IFN response was to establish whether this was in fact a response to IFNs, i.e. was there an increase in the IFNs level after CBL0137 treatment. However, our attempts to detect IFNs (alpha, beta or gamma) in plasma of mice treated with CBL0137 or in cell culture medium failed. This may be due to the short half-life and/or low levels of IFNs even after induction. To overcome this limitation and to test whether the induction of IFN responsive transcription after CBL0137 treatment was due to IFNs, we used cells with different components of the IFN signaling pathway inactivated, such as MEF from mice with a knockout of type I IFN receptor (Ifnar) or a transcription factor controlling the expression of IFN responsive genes in response to IFN, Irf1 (MEF from mice with knockout of Irf1) or Irf7 (MEF transduced with shRNA to Irf7). We also used p53 -/- MEF since we have shown previously that the absence of p53 increases IFN signaling in response to dsRNA (Leonova et al., 2013). A deficiency in either Ifnar and Irf7 reduced or completely eliminated

induction of Ifit3 expression after CBL0137, respectively. In contrast, the loss of p53 stimulated the response. There was no effect of Irf1 knockout (Fig.5A). Similar results were obtained *in vivo* using spleens from Ifnar-/-, Irf7-/- or p53-/- mice treated with CBL0137 (Fig.5B).

CBL0137 treatment leads to transcription of repetitive heterochromatic genomic regions

A known trigger of the IFN response is a viral infection. There are several ways by which cells can detect viral invasion. First, viral dsRNA can be detected by several intra-cellular receptors, such as TLR3, 7 or 8, RIG1 and MDA5 (rev. in (Unterholzner, 2013)). Additionally, the presence of DNA in the cytoplasm or non-B DNA, such as left handed Z-DNA, found in some viruses (Nordheim & Rich, 1983) can also be recognized by cell as viral infection. In the latter case, the IFN response is activated via Z-DNA-binding protein 1 (ZBP1), also known as DNA-dependent activator of IFN (DAI) (Takaoka, Wang et al., 2007). Importantly, we have recently shown that high doses of CBL0137 caused disassembly of nucleosomes in cells, which led to the extensive negative supercoiling of DNA and a transition of B-DNA into left-handed Z-DNA (Fleyshman, Prendergast et al., 2017). Although this effect was observed at significantly higher CBL0137 concentrations (>2.5□M) than that which induced an IFN response, we investigated whether the effect of CBL0137 on nucleosomes could be responsible for its effect on the IFN response. To do this, we deleted the ZBP1 gene from Hela and HT1080 cells using CRISP/Cas9 recombinase and two human ZBP1gRNAs. The loss of ZBP1 expression was confirmed by RT-PCR (Fig. S6A). We compared the effect of CBL0137 on ISRE-mCherry reporter activity in these cells to wild type cells and cells transduced with control gRNA, and observed no change in the induction of the reporter activity 48 hours after CBL0137 treatment (Fig.S6B). There was also no Z-DNA present in the cells treated with at CBL0137 doses that caused a robust IFN response as judged by the absence of staining with Z-DNA antibodies (Fig.S6C).

We next determined whether dsRNA induced an IFN response in CBL0137-treated cells. Using an antibody to dsRNA (Targett-Adams, Boulant et al., 2008), we observed increased staining in CBL0137-treated cells (Fig. 6A, B). One potential endogenous source of dsRNA may be from the transcription of repetitive elements, such as endogenous retroviruses, centromeric, or pericentromeric repeats (Leonova et al., 2013). Transcription of these elements may be enhanced as a result of nucleosome destabilization and chromatin unfolding caused by CBL0137. Short Interspersed Nuclear Element (SINE) retrotransposons constitute one of the main components of the genomic repetitive fraction (Kramerov & Vassetzky, 2011). Hence, we first tested whether transcription of B1 SINE is increased upon CBL0137 treatment using northern blotting. In samples of untreated MEFs, binding of the B1 probe was detected for a number of different length transcripts, possibly due to the presence of B1 repeats within the introns of multiple mRNAs. After CBL0137 treatment, a single lower molecular weight band that was strongly bound by the B1 probe appeared, which was similar in size and abundance to the band in cells treated with the positive control (5-aza-cytidine (5-aza)) (Fig. 6C). To determine whether other transcripts that are able to form dsRNAs appear in cells treated with CBL0137, we performed RNA-sequencing (RNA-seq) analysis using total RNA from wild type and p53-/- MEF treated with CBL0137 *in vitro* or lungs from mice collected 24 hours after treatment with 60 mg/kg CBL0137 *in vivo*. This analysis demonstrated a significant increase in the number of transcripts corresponding to several classes of endogenous viruses as well as GSAT (pericentromeric) and SATMIN (centromeric) repeats in cells (Fig.6D and Table S7). These data suggest that treatment with CBL0137 leads to the activation of the transcription of heterochromatic regions, which are not or minimally transcribed under basal conditions.

TRAIN occurs in response to nucleosome "opening"

CBL0137 may induce transcription of genomic regions that are silenced at physiological conditions via several different mechanisms. Loss of FACT via c-trapping may lead to activation of silenced transcription since mutations of FACT subunits in yeast causes transcription from cryptic sites that are covered by nucleosomes in basal conditions (Mason & Struhl, 2003), (Jamai, Puglisi et al., 2009). FACT is also important for chromatin assembly at centromeres (Okada, Okawa et al., 2009, Prendergast, Muller et al., 2016). We observed the induction of the IFN response in organs that lacked FACT (lung and liver); however, the absence of FACT in these tissues does not exclude the role of FACT in the prevention of the response. However, it was clear that there are FACT independent effects of CBL0137 on transcription.

Opening or disassembly of nucleosomes due to CBL0137 binding to DNA may increase accessibility of DNA to RNA Polymerase (RNAP) II. To see whether CBL0137 can induce transcription of a reporter silenced due to chromatin condensation, we used HeLa-TI cells described in (Poleshko et al., 2010, Shalginskikh et al., 2013) and containing integrated avian sarcoma genome with silent green fluorescent protein (GFP) gene. Under basal conditions, GFP is expressed in very few cells; however, the opening of chromatin using the HDAC inhibitor trichostatin A (TSA) activates GFP expression in significant proportion of cells (Fig.7A). Increase in proportion of GFP expressing cells was observed after CBL0137 treatment (Fig. 7A). Moreover, effect of CBL0137 was faster than TSA, reaching maximum in 12 hours, while after TSA, peak of GFP expression was reached at 36 hours.

Next, we tested whether chromatin opening by HDAC inhibition caused TRAIN. We treated MEF and HeLa-TI cells with TSA, CBL0137, and monitored the activation of IFN signaling by RT-PCR in MEF or ISRE-mCherry reporter in Hela-TI cells (Fig. 7B, C). In MEF cells both agents, TSA and CBL0137, induced expression of Ifit3 and Irf7 genes (Fig.7B), while in HeLa-TI cells, robust induction of ISRE reporter was evident only after CBL0137 treatment. TSA caused a weak increase in ISRE reporter activity (1.5 folds versus >5 folds in case of CBL0137) only at the highest concentration (500nM, Fig.7C) when evidence of toxicity was present. At the same time, the degree of activation of the silenced GFP in HeLa-TI cells was similar for TSA and CBL0137 (Fig.7C). Thus, TRAIN can be induced by different means of chromatin opening, but its magnitude depends on cell type.

Importantly, although GFP expression was increased by both agents, the mechanisms of chromatin opening were different for TSA and CBL0137. As expected TSA treatment caused an increase in the amount of acetylated histone H3, while CBL0137 - a decrease in the amount of chromatin-bound histone H3 (Fig.7D). However, as we saw previously (Safina et al., 2017), substantial loss of core histones, i.e. chromatin disassembly, was observed at CBL0137 concentration ~5μM, which is much higher than concentrations at which we observed TRAIN (<1 μM, peak at 0.5 μM). We proposed that nucleosome "opening", i.e. state of loose contact of DNA and histone core without loss of histones from the core (proposed in the review (Zlatanova, Bishop et al., 2009)) is enough for the induction of TRAIN, i.e. no nucleosome disassembly or dissociation of nucleosome parts is needed. Although these is no clear definition of opened and closed nucleosome state, in cells closed nucleosome is additionally "locked" with linker histone H1 (Syed, Goutte-Gattat et al., 2010, Zhou, Feng et al., 2013). Thus we decided to see how distribution of H1 is changed upon treatment with CBL0137 using imaging of live cell expressing m-Cherry tagged histone H1.5. CBL0137 treatment led to redistribution of H1.5 from chromatin to nucleoli, similarly to the effect of CBL0137 on core histones (Safina et al., 2017) , but

observed faster and at much lower concentrations of CBL0137 (Fig.8A, B). TRAIN in CBL0137 treated cells was observed at the same concentration range as redistribution of histone H1 and before disassembly of nucleosome core, suggesting that nucleosome opening is sufficient to allow transcription of heterochromatic regions in cells.

TRAIN induced by CBL0137 impacts the tumor-preventive activity of CBL0137

We have previously shown that administration of CBL0137 to tumor prone mice prior to tumor onset significantly reduced the incidence of cancer and diminished the occurrence of aggressive forms of breast cancer (Koman, Commane et al., 2012). We explained this effect by the fact that CBL0137 inhibited NF-kappaB and activated p53, both well-established mechanisms of cancer prevention (rev. in (Athar, Elmets et al., 2011) and (Lin, Bai et al., 2010)). However, activation of IFN may be an additional mechanism to eliminate transformed cells, because they are more sensitive to IFN-mediated apoptosis than normal cells (rev. in (Parker, Rautela et al., 2016)). To test this hypothesis, we used p53-negative MEF (to eliminate the effect of p53 activation) with a functional or disabled IFN response via knockout of Ifnar (Picaud, Bardot et al., 2002). MEF cells have almost no basal NF-kappaB activity. Both cell types were transduced with a lentiviral construct for the expression of mutant H-Ras^{V12} oncogene. Forty-eight hours after lentiviral transduction, cells were treated with a low dose of CBL0137 for an additional 48 hours, and then left to grow in drug-free medium. After 10 days, the number of transformed foci was significantly reduced in cells treated with CBL0137 compared to untreated cells, but only if the cells had functional INF receptor (Ifnar +/+, Fig.9). Thus, TRAIN may be an additional mechanism by which CBL0137 exerts its anti-tumor and tumor preventive effect.

Discussion

Our study describes the consequences of chromatin destabilization caused by small molecule binding to DNA. CBL0137 was identified in a cell based screening, and some of its effects, such as activation of p53 and inhibitions of NF-kappaB, functional inactivation of FACT, higher toxicity to tumor, than normal cells were already described (Gasparian et al., 2011), (Barone, Burkhart et al., 2017, Carter et al., 2015, Dermawan et al., 2016). However, recently we demonstrated that binding of CBL0137 to DNA destabilizes nucleosome *in vitro* and *in vivo* and leads to histone eviction and chromatin decondensation in cells (Safina et al., 2017). Since CBL0137 does not cause chemical DNA modifications and has no effect on transcription and replication of naked DNA *in vitro* at concentrations used in this study, this creates a unique situation to assess how chromatin “damage” influences transcription.

First, we would like to define chromatin “damage” as artificially induced with a drug change in original chromatin composition. In case of CBL0137 it occurs most probably in few continuous phases (Fig.10): at lower concentrations of CBL0137 (<1μM in cells) nucleosome “opens”, loses linker histone H1 without dissociation and loss of core histones, at higher concentrations (1-5 μM) – dimer detachment may occur with occasional loss of core histones. We clearly saw this stage *in vitro* as appearance of hexasome (Safina et al., 2017). At concentrations >5 μM nucleosome is disassembled and core histones are evicted from chromatin. This sequence of events is in line with reversibility of CBL0137 toxic effects: after short incubation with < 1 μM of CBL0137 cells can be washed from the drug with almost no harm, cells incubated with 1-3 μM for no more than 1 hour survive with some loss of viability, however >5 μM present for more than 15 minutes – lead to complete cell death in line with complete disassembly of their

chromatin. An important and completely unknown question is what actually causes cell death upon loss of chromatin integrity.

Other cellular "responses" to CBL0137 treatment are also aligned with gradual change in nucleosome organization. The first cellular factor, which we found, "reacting" to the problems with chromatin packaging in CBL0137 treated cells was histone chaperone FACT, undergoing chromatin trapping in response to nucleosome disassembly. It was shown that human FACT cannot bind and uncoil "closed" nucleosome (Tsunaka, Fujiwara et al., 2016, Valieva, Gerasimova et al., 2017) (Fig.10). However, nucleosome opening most probably allows FACT to invade nucleosome and bind H3/H4 tetramer via middle domain of SPT16 and H2A/H2B dimer via c-terminal parts of both subunits (Belotserkovskaya et al., 2003, Kemble, McCullough et al., 2015, Tsunaka et al., 2016, Winkler & Luger, 2011). In cells we see this as SPT16-mediated "n (nucleosome)-trapping" observed at 0.3-1μM of CBL0137. Concentrations >3μM due to nucleosome disassembly significant negative supercoiling caused base-unpairing of DNA and transition of B-DNA into left-handed Z-form, which FACT binds via c-terminal intrinsically disordered domain of SSRP1 subunit (Safina et al., 2017). FACT has a plethora of activities related to transcription (rev. in (Reinberg & Sims, 2006)); therefore many of CBL0137 effects on transcription might be explained via functional inactivation of FACT. However, we suspected that opening of chromatin may have consequences independent on FACT.

The most prominent and uniform change observed in the presence and absence of FACT was activation of IFN response in all tested organs and cells on mRNA and protein levels. Induction of IFN sensitive genes (ISG) has bell-shaped curve, with maximum increase at the concentration of CBL0137 (~0.5μM) coresponding nucleosome "opening", followed by inhibition of transcription at concentrations higher than 1μM when nucleosome disassembly starts. We believe that IFN is activated in response to dsRNA formed due to the increased transcription from normally silenced heterochromatic regions. There was a report proposing the role of histone H1 in the silencing of ISGs: knockdown of H1 chaperone TAF1 in cells resulted in H1 loss from ISG promoters and activation of their transcription (Kadota & Nagata, 2014). However, the set of data in the report of (Kadota & Nagata, 2014) does not exclude the role of general chromatin decondensation due to the reduction of H1 deposition into heterochromatin. We showed that in case of CBL0137 treatment, transcription of ISGs is abrogated if IFN signaling pathway is disabled (e.g. Ifnar-/- cells and mice), suggesting that there is no direct effect of CBL0137 on the promoters of ISGs. If we assume, that IFN is activated in response to increase in transcription of repetitive heterochromatin genomic regions, then the puzzling and intriguing question is why nucleosome "opening" is accompanied by selective activation of transcription of these elements, but not most of genes, while nucleosome disassembly leads to the inhibition of transcription genome-wide. We propose that displacement of histone H1 may make heterochromatin accessible for RNA polymerase, while accessibility of genomic regions not locked with H1 does not change. Inhibition may be explained by direct effect of higher concentrations of the compound, bound to DNA, on RNA polymerases activity, but this requires further investigation.

Importantly anti-cancer effect in mice is seen at concentrations activating IFN response, suggesting that chromatin opening without chromatin disassembly is enough to cause anti-cancer effect *in vivo*. This also opens opportunity to use some of IFN responsive factor as pharmacodynamic markers of curaxin's activity in clinic, since many of these factors are secreted and were detected in plasma of mice.

Thus, curaxins, compounds with established anti-cancer activity in multiple preclinical models may be also used as a tool to affect chromatin organization and folding globally in cells and animals to study consequences of abrupt loss of epigenetic regulation *in vivo*. Potentially, this property of curaxins may be useful for reprogramming and other types of therapeutic epigenetic manipulations.

One more aspect of this study is in expanding of the set of situations when TRAIN response occurs. Before, we and others observed it upon loss of DNA methylation (Leonova et al., 2013), (Chiappinelli et al., 2015, Guryanova et al., 2016, Roulois et al., 2015). and mostly in case of p53 deficiency (Leonova et al., 2013). Here we see that general chromatin decondensation due to nucleosome opening is also accompanied by TRAIN with much less dependence of p53 status. We dare to propose that TRAIN may be more general response to the problems with chromatin packaging and the danger of loss of epigenetic integrity. Stability of cell differentiation status, which can still be easily detected even in Hela cells, after more than 60 years in culture, is a long-standing puzzle. Theoretically, it can be ensured either by stability and low rate of mistake in replication of chromatin marks or by auto-regulatory mechanism of elimination of cells with loss of epigenetic information, similar to p53-dependent apoptosis in response to DNA damage. It is tempting to speculate that TRAIN may be such mechanism, triggered by elevation of expression of silenced repetitive genomic elements and executed by IFN response, capable of killing cells. Most probably this mechanism evolved in response to real viral threat, and especially in the form of expansion of endogenous retroviral elements, but eventually started to serve as an epigenetic lock, which may be as beneficial (support of differentiation state), as well as limiting cell plasticity and therefore ability to transdifferentiate and regenerate organs and tissues.

References

Athar M, Elmets CA, Kopelovich L (2011) Pharmacological activation of p53 in cancer cells. Curr Pharm Des 17: 631-9

Barone TA, Burkhart CA, Safina A, Haderski G, Gurova KV, Purmal AA, Gudkov AV, Plunkett RJ (2017) Anticancer drug candidate CBL0137, which inhibits histone chaperone FACT, is efficacious in preclinical orthotopic models of temozolomide-responsive and -resistant glioblastoma. Neuro Oncol 19: 186-196

Belotserkovskaya R, Oh S, Bondarenko VA, Orphanides G, Studitsky VM, Reinberg D (2003) FACT facilitates transcription-dependent nucleosome alteration. Science 301: 1090-3

Brzostek-Racine S, Gordon C, Van Scoy S, Reich NC (2011) The DNA damage response induces IFN. J Immunol 187: 5336-45

Campos EI, Stafford JM, Reinberg D (2014) Epigenetic inheritance: histone bookmarks across generations. Trends Cell Biol 24: 664-74

Carter DR, Murray J, Cheung BB, Gamble L, Koach J, Tsang J, Sutton S, Kalla H, Syed S, Gifford AJ, Issaeva N, Biktasova A, Atmadibrata B, Sun Y, Sokolowski N, Ling D, Kim PY, Webber H, Clark A, Ruhle M et al. (2015) Therapeutic targeting of the MYC signal by inhibition of histone chaperone FACT in neuroblastoma. Sci Transl Med 7: 312ra176

Chiappinelli KB, Strissel PL, Desrichard A, Li H, Henke C, Akman B, Hein A, Rote NS, Cope LM, Snyder A, Makarov V, Budhu S, Slamon DJ, Wolchok JD, Pardoll DM, Beckmann MW, Zahnow CA, Merghoub T, Chan TA, Baylin SB et al. (2015) Inhibiting DNA Methylation Causes an Interferon Response in Cancer via dsRNA Including Endogenous Retroviruses. Cell 162: 974-86

Dermawan JK, Hitomi M, Silver DJ, Wu Q, Sandlesh P, Sloan AE, Purmal AA, Gurova KV, Rich JN, Lathia JD, Stark GR, Venere M (2016) Pharmacological Targeting of the Histone Chaperone Complex FACT Preferentially Eliminates Glioblastoma Stem Cells and Prolongs Survival in Preclinical Models. Cancer Res 76: 2432-42

Ebrahimi B (2015) Reprogramming barriers and enhancers: strategies to enhance the efficiency and kinetics of induced pluripotency. Cell Regen (Lond) 4: 10

Fleyshman D, Prendergast L, Safina A, Paszkiewicz G, Commane M, Morgan K, Attwood K, Gurova K (2017) Level of FACT defines the transcriptional landscape and aggressive phenotype of breast cancer cells. Oncotarget 8: 20525-20542

Garcia H, Fleyshman D, Kolesnikova K, Safina A, Commane M, Paszkiewicz G, Omelian A, Morrison C, Gurova K (2011) Expression of FACT in mammalian tissues suggests its role in maintaining of undifferentiated state of cells. Oncotarget 2: 783-96

Gariglio M, Ying GG, Hertel L, Gaboli M, Clerc RG, Landolfo S (1997) The high-mobility group protein T160 binds to both linear and cruciform DNA and mediates DNA bending as determined by ring closure. Exp Cell Res 236: 472-81

Gasparian AV, Burkhart CA, Purmal AA, Brodsky L, Pal M, Saranadasa M, Bosykh DA, Commane M, Guryanova OA, Pal S, Safina A, Sviridov S, Koman IE, Veith J, Komar AA, Gudkov AV, Gurova KV (2011) Curaxins: anticancer compounds that simultaneously suppress NF-kappaB and activate p53 by targeting FACT. Sci Transl Med 3: 95ra74

Guryanova OA, Shank K, Spitzer B, Luciani L, Koche RP, Garrett-Bakelman FE, Ganzel C, Durham BH, Mohanty A, Hoermann G, Rivera SA, Chramiec AG, Pronier E, Bastian L, Keller MD, Tovbin D, Loizou E, Weinstein AR, Gonzalez AR, Lieu YK et al. (2016) DNMT3A mutations promote anthracycline resistance in acute myeloid leukemia via impaired nucleosome remodeling. Nat Med 22: 1488-1495

Hussein SM, Nagy AA (2012) Progress made in the reprogramming field: new factors, new strategies and a new outlook. Curr Opin Genet Dev 22: 435-43

Imam AM, Ackrill AM, Dale TC, Kerr IM, Stark GR (1990) Transcription factors induced by interferons alpha and gamma. Nucleic Acids Res 18: 6573-80

Jamai A, Puglisi A, Strubin M (2009) Histone chaperone spt16 promotes redeposition of the original h3-h4 histones evicted by elongating RNA polymerase. Mol Cell 35: 377-83

Kadota S, Nagata K (2014) Silencing of IFN-stimulated gene transcription is regulated by histone H1 and its chaperone TAF-I. Nucleic Acids Res 42: 7642-53

Kapitonov VV, Jurka J (2008) A universal classification of eukaryotic transposable elements implemented in Repbase. Nat Rev Genet 9: 411-2; author reply 414

Kemble DJ, McCullough LL, Whitby FG, Formosa T, Hill CP (2015) FACT Disrupts Nucleosome Structure by Binding H2A-H2B with Conserved Peptide Motifs. Mol Cell 60: 294-306

Koman IE, Commane M, Paszkiewicz G, Hoonjan B, Pal S, Safina A, Toshkov I, Purmal AA, Wang D, Liu S, Morrison C, Gudkov AV, Gurova KV (2012) Targeting FACT complex suppresses mammary tumorigenesis in Her2/neu transgenic mice. Cancer Prev Res (Phila) 5: 1025-35

Kramerov DA, Vassetzky NS (2011) SINEs. Wiley Interdiscip Rev RNA 2: 772-86

Krohn NM, Stemmer C, Fojan P, Grimm R, Grasser KD (2003) Protein kinase CK2 phosphorylates the high mobility group domain protein SSRP1, inducing the recognition of UV-damaged DNA. J Biol Chem 278: 12710-5

Kulaeva OI, Draghici S, Tang L, Kraniak JM, Land SJ, Tainsky MA (2003) Epigenetic silencing of multiple interferon pathway genes after cellular immortalization. Oncogene 22: 4118-27

Leonova KI, Brodsky L, Lipchick B, Pal M, Novototskaya L, Chenchik AA, Sen GC, Komarova EA, Gudkov AV (2013) p53 cooperates with DNA methylation and a suicidal interferon response to maintain epigenetic silencing of repeats and noncoding RNAs. Proc Natl Acad Sci U S A 110: E89-98

Lin Y, Bai L, Chen W, Xu S (2010) The NF-kappaB activation pathways, emerging molecular targets for cancer prevention and therapy. Expert Opin Ther Targets 14: 45-55

Luger K, Mader AW, Richmond RK, Sargent DF, Richmond TJ (1997) Crystal structure of the nucleosome core particle at 2.8 A resolution. Nature 389: 251-60

Mason PB, Struhl K (2003) The FACT complex travels with elongating RNA polymerase II and is important for the fidelity of transcriptional initiation in vivo. Mol Cell Biol 23: 8323-33

Miller KM (2010) Advances in understanding genome maintenance. Genome Biol 11: 301

Miska EA, Ferguson-Smith AC (2016) Transgenerational inheritance: Models and mechanisms of non-DNA sequence-based inheritance. Science 354: 59-63

Mruk DD, Cheng CY (2015) The Mammalian Blood-Testis Barrier: Its Biology and Regulation. Endocr Rev 36: 564-91

Nordheim A, Rich A (1983) Negatively supercoiled simian virus 40 DNA contains Z-DNA segments within transcriptional enhancer sequences. Nature 303: 674-9

Okada M, Okawa K, Isobe T, Fukagawa T (2009) CENP-H-containing complex facilitates centromere deposition of CENP-A in cooperation with FACT and CHD1. Mol Biol Cell 20: 3986-95

Parker BS, Rautela J, Hertzog PJ (2016) Antitumour actions of interferons: implications for cancer therapy. Nat Rev Cancer 16: 131-44

Patro R, Mount SM, Kingsford C (2014) Sailfish enables alignment-free isoform quantification from RNA-seq reads using lightweight algorithms. Nat Biotechnol 32: 462-4

Pfeffer LM (2011) The role of nuclear factor kappaB in the interferon response. J Interferon Cytokine Res 31: 553-9

Picaud S, Bardot B, De Maeyer E, Seif I (2002) Enhanced tumor development in mice lacking a functional type I interferon receptor. J Interferon Cytokine Res 22: 457-62

Poleshko A, Einarson MB, Shalginskikh N, Zhang R, Adams PD, Skalka AM, Katz RA (2010) Identification of a functional network of human epigenetic silencing factors. J Biol Chem 285: 422-33

Prendergast L, Muller S, Liu Y, Huang H, Dingli F, Loew D, Vassias I, Patel DJ, Sullivan KF, Almouzni G (2016) The CENP-T/-W complex is a binding partner of the histone chaperone FACT. Genes Dev 30: 1313-26

Qian HR, Huang S (2005) Comparison of false discovery rate methods in identifying genes with differential expression. Genomics 86: 495-503

Reinberg D, Sims RJ, 3rd (2006) de FACTo nucleosome dynamics. J Biol Chem 281: 23297-301

Roulois D, Loo Yau H, Singhania R, Wang Y, Danesh A, Shen SY, Han H, Liang G, Jones PA, Pugh TJ, O'Brien C, De Carvalho DD (2015) DNA-Demethylating Agents Target Colorectal Cancer Cells by Inducing Viral Mimicry by Endogenous Transcripts. Cell 162: 961-73

Safina A, Cheney P, Pal M, Brodsky L, Ivanov A, Kirsanov K, Lesovaya E, Naberezhnov D, Nesher E, Koman I, Wang D, Wang J, Yakubovskaya M, Winkler D, Gurova K (2017) FACT is a sensor of DNA torsional stress in eukaryotic cells. Nucleic Acids Res 45: 1925-1945

Safina A, Garcia H, Commane M, Guryanova O, Degan S, Kolesnikova K, Gurova KV (2013) Complex mutual regulation of facilitates chromatin transcription (FACT) subunits on both mRNA and protein levels in human cells. Cell Cycle 12: 2423-34

Shalginskikh N, Poleshko A, Skalka AM, Katz RA (2013) Retroviral DNA methylation and epigenetic repression are mediated by the antiviral host protein Daxx. J Virol 87: 2137-50

Silin DS, Lyubomska OV, Ershov FI, Frolov VM, Kutsyna GA (2009) Synthetic and natural immunomodulators acting as interferon inducers. Curr Pharm Des 15: 1238-47

Syed SH, Goutte-Gattat D, Becker N, Meyer S, Shukla MS, Hayes JJ, Everaers R, Angelov D, Bednar J, Dimitrov S (2010) Single-base resolution mapping of H1-nucleosome interactions and 3D organization of the nucleosome. Proc Natl Acad Sci U S A 107: 9620-5

Takaoka A, Wang Z, Choi MK, Yanai H, Negishi H, Ban T, Lu Y, Miyagishi M, Kodama T, Honda K, Ohba Y, Taniguchi T (2007) DAI (DLM-1/ZBP1) is a cytosolic DNA sensor and an activator of innate immune response. Nature 448: 501-5

Targett-Adams P, Boulant S, McLauchlan J (2008) Visualization of double-stranded RNA in cells supporting hepatitis C virus RNA replication. J Virol 82: 2182-95

Tsunaka Y, Fujiwara Y, Oyama T, Hirose S, Morikawa K (2016) Integrated molecular mechanism directing nucleosome reorganization by human FACT. Genes Dev 30: 673-86

Unterholzner L (2013) The interferon response to intracellular DNA: why so many receptors? Immunobiology 218: 1312-21

Valieva ME, Armeev GA, Kudryashova KS, Gerasimova NS, Shaytan AK, Kulaeva OI, McCullough LL, Formosa T, Georgiev PG, Kirpichnikov MP, Studitsky VM, Feofanov AV (2016) Large-scale ATP-independent nucleosome unfolding by a histone chaperone. Nat Struct Mol Biol 23: 1111-1116

Valieva ME, Gerasimova NS, Kudryashova KS, Kozlova AL, Kirpichnikov MP, Hu Q, Botuyan MV, Mer G, Feofanov AV, Studitsky VM (2017) Stabilization of Nucleosomes by Histone Tails and by FACT Revealed by spFRET Microscopy. Cancers (Basel) 9

Wagner GP, Kin K, Lynch VJ (2013) A model based criterion for gene expression calls using RNA-seq data. Theory Biosci 132: 159-64

Wang J, Lindahl T (2016) Maintenance of Genome Stability. Genomics Proteomics Bioinformatics 14: 119-21

Wathelet MG, Lin CH, Parekh BS, Ronco LV, Howley PM, Maniatis T (1998) Virus infection induces the assembly of coordinately activated transcription factors on the IFN-beta enhancer in vivo. Mol Cell 1: 507-18

Winkler DD, Luger K (2011) The histone chaperone FACT: structural insights and mechanisms for nucleosome reorganization. J Biol Chem 286: 18369-74

Wu TF, Chu DS (2008) Sperm chromatin: fertile grounds for proteomic discovery of clinical tools. Mol Cell Proteomics 7: 1876-86

Yarnell AT, Oh S, Reinberg D, Lippard SJ (2001) Interaction of FACT, SSRP1, and the high mobility group (HMG) domain of SSRP1 with DNA damaged by the anticancer drug cisplatin. J Biol Chem 276: 25736-41

Zhou BR, Feng H, Kato H, Dai L, Yang Y, Zhou Y, Bai Y (2013) Structural insights into the histone H1-nucleosome complex. Proc Natl Acad Sci U S A 110: 19390-5

Zlatanova J, Bishop TC, Victor JM, Jackson V, van Holde K (2009) The nucleosome family: dynamic and growing. Structure 17: 160-71

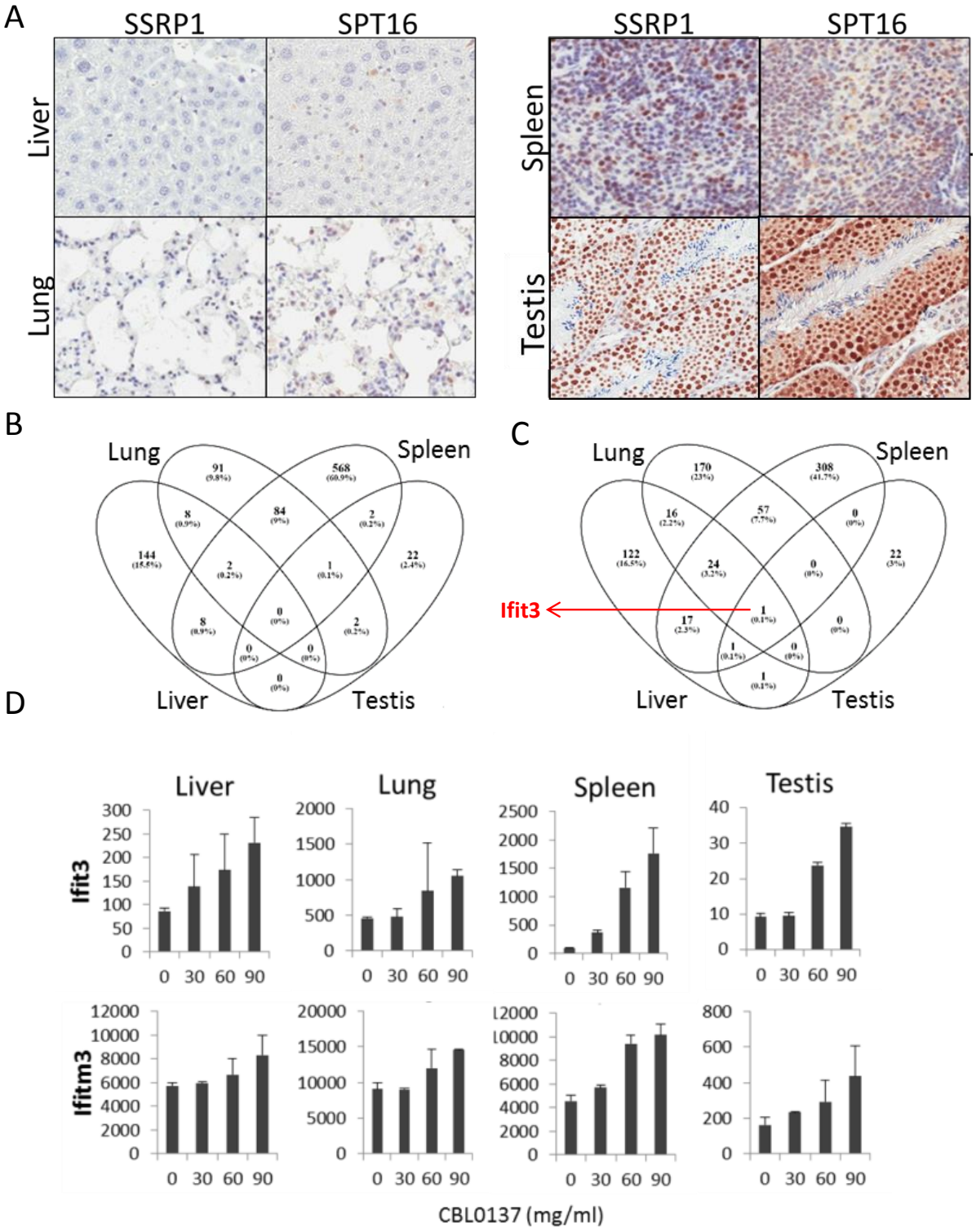

Figure 1. Effect of CBL0137 on transcription of genes in FACT positive and negative mouse tissues. A. IHC staining with SSRP1 antibody of liver and lung tissues with no detectable SSRP1 and spleen and testis expressing SSRP1. B, C. Venn diagrams of the lists of genes which expression was downregulated (B) or upregulated (C) in response to CBL0137. D. Dose-dependent upregulation of Ifit3 and Ifitm3 mRNAs in different organs. Mean normalized value of microarray hybridization signal +/- SD.

A

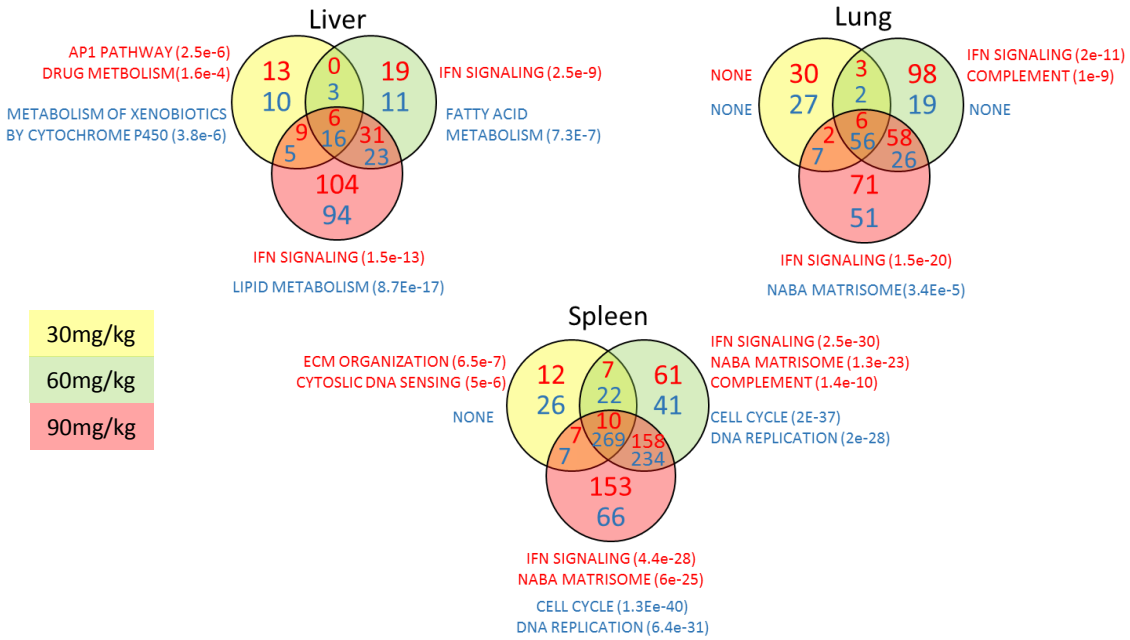

B

Gene Set Name	# Genes in Gene Set (K)	# Genes in Overlap (k)	k/K	p-value	FDR q-value
REACTOME_INTERFERON_ALPHA_BETA_SIGNALING	64	14	0.2188	1.44E-26	1.91E-23
REACTOME_INTERFERON_SIGNALING	159	16	0.1006	1.76E-24	1.17E-21
REACTOME_CYTOKINE_SIGNALING_IN_IMMUNE_SYSTEM	270	17	0.063	2.00E-22	8.84E-20
REACTOME_IMMUNE_SYSTEM	933	23	0.0247	5.60E-21	1.86E-18
REACTOME_INTERFERON_GAMMA_SIGNALING	63	6	0.0952	1.05E-09	2.80E-07
REACTOME_REGULATION_OF_IFNA_SIGNALING	24	4	0.1667	7.15E-08	1.58E-05
ST_TYPE_I_INTERFERON_PATHWAY	9	3	0.3333	3.62E-07	5.81E-05
REACTOME_INNATE_IMMUNE_SYSTEM	279	7	0.0251	4.31E-07	5.81E-05
PID_IL23_PATHWAY	37	4	0.1081	4.38E-07	5.81E-05

C

Gene Set Name	# Genes in Gene Set (K)	Transcriptional targets of	# Genes in Overlap (k)	k/K	p-value	FDR q-value
V$ISRE_01	247	STAT1	10	0.0405	1.17E-11	7.21E-09
STTTCRNTTT_V$IRF_Q6	188	Unknown	8	0.0426	1.00E-09	3.09E-07
V$IRF_Q6	242	IRF1	8	0.0331	7.29E-09	1.36E-06
V$ICSBP_Q6	248	IRF8	8	0.0323	8.83E-09	1.36E-06
V$IRF7_01	252	IRF7	6	0.0238	4.06E-06	5.00E-04
TGANTCA_V$AP1_C	1121	JUN	9	0.008	9.76E-05	1.00E-02
YATGNWAAT_V$OCT_C	360	Unknown	5	0.0139	3.36E-04	2.95E-02

Figure 2. Activation of IFN response is detected in response to CBL0137 in different tissues of mice via GSEA. A. Venn diagrams showing number of up (red font) or down (blue font) regulated genes in response to CBL0137 together with gene set names enriched for these genes. P-value of overlap is shown in parentheses. B. GSEA of curated signaling pathways using the list of genes upregulated in two or more tissues in response to CBL0137. C. GSEA of targets of known transcriptional factors using list of genes upregulated in all tissues in response to CBL0137.

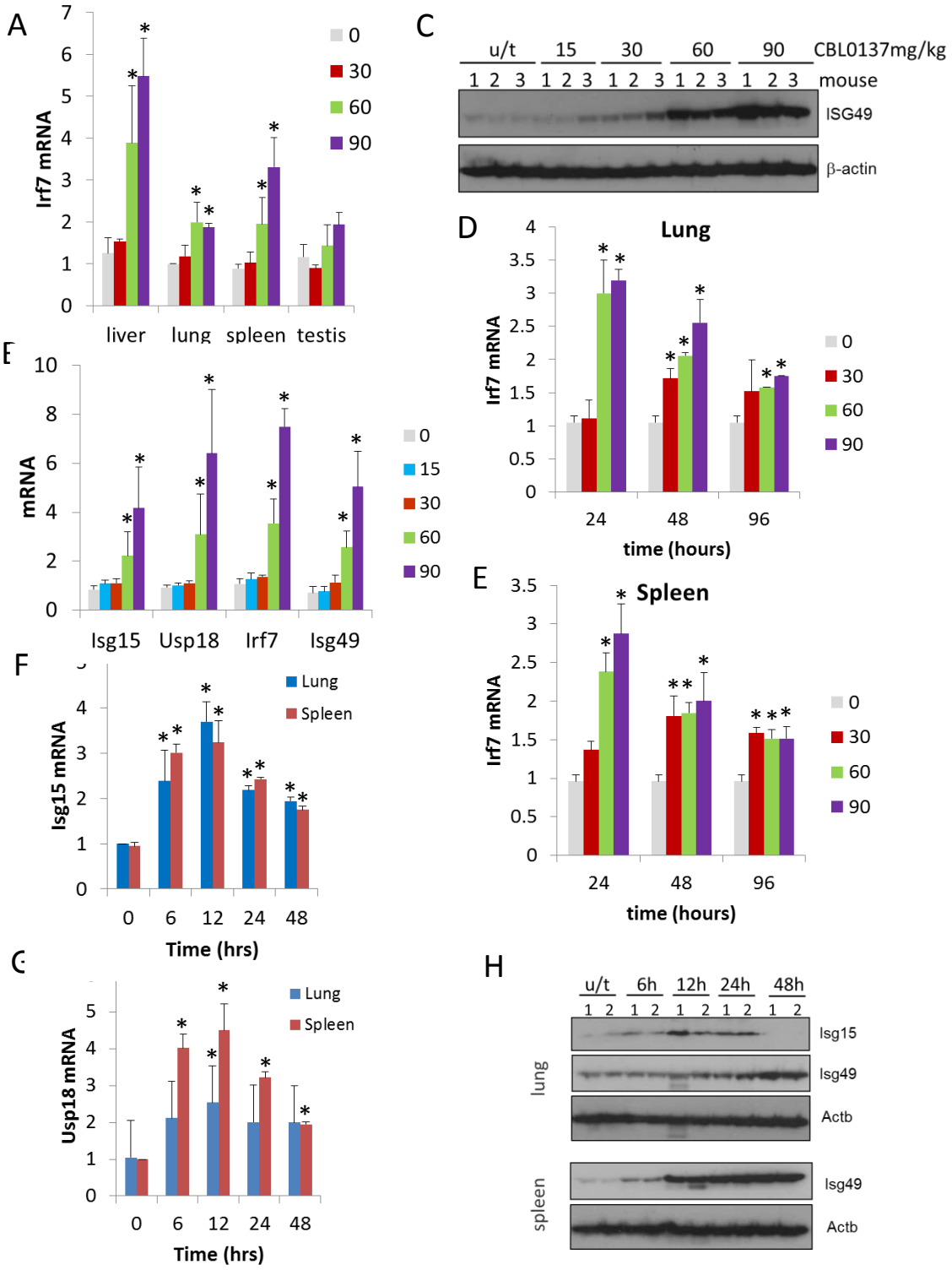

Figure 3. CBL0137 treatments leads to the increase in expression of IFN responsive genes in different tissues of mice. Quantitation of RT-PCR data (A, B, D, E, F, G) shown as fold change upon treatment with different doses of CBL0137 (in mg/kg) comparing to vehicle treated control. Mean values from three mice +/-SD. Immunoblotting of mouse plasma (C) or tissue lysates (H). A. 24 hours treatment of C57Bl/6 mice. B and C. 24 hours treatment of NIH Swiss mice. D - H. Different time treatment of C57Bl/6 mice.

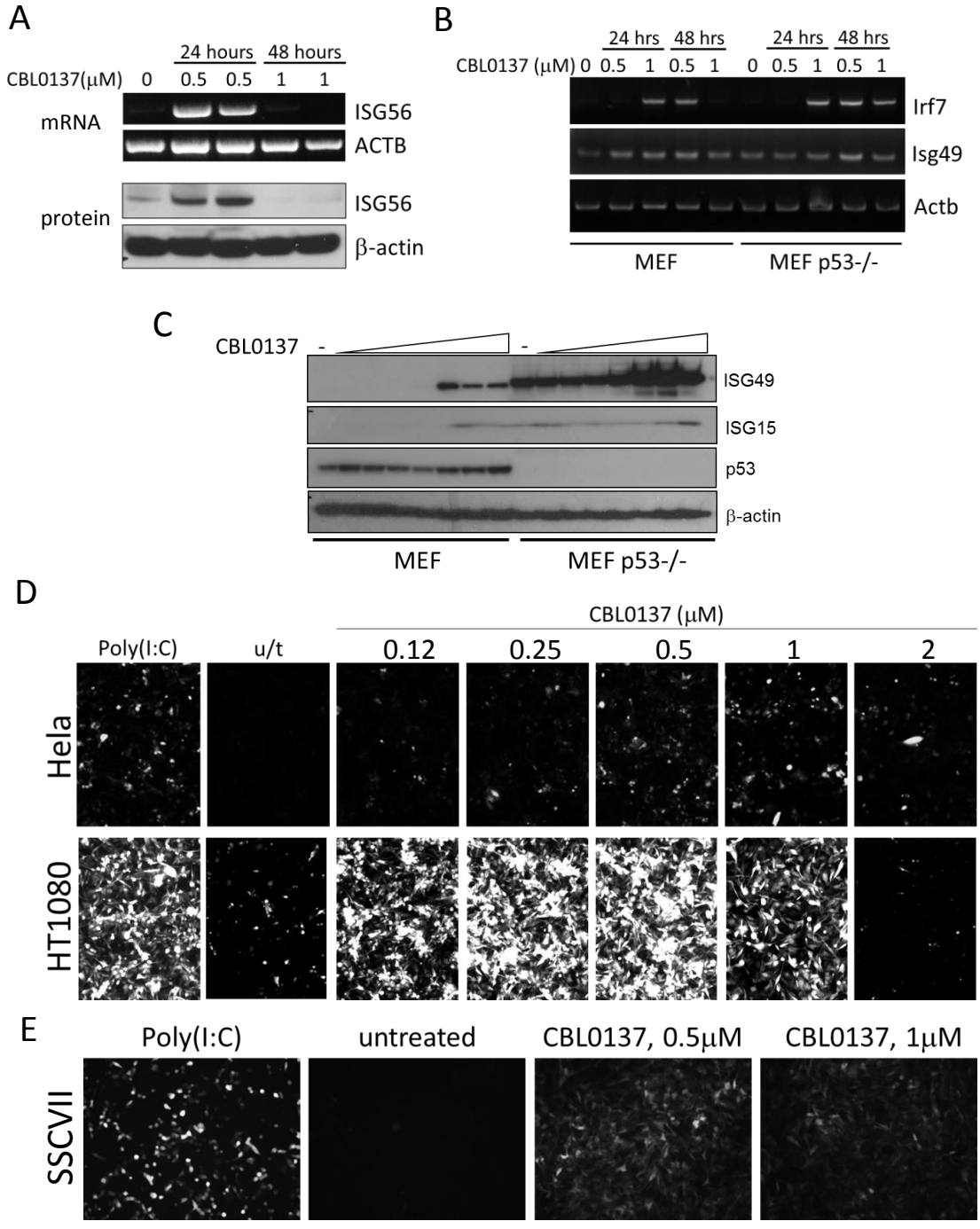

Figure 4. Induction of IFN response in human and mouse cells in vitro treated with CBL0137. A. RT-PCR and immunoblotting of mRNA and lysates from human diploid fibroblasts. ISG56 is a product of human IFIT3 gene. B. RT-PCR of RNA from MEF, wild type of p53 deficient. C. Immunoblotting of lysate of MEF treated with different doses of CBL0137 (0.03 – 2μM) for 24 hours. D and E. Microphotographs of human (D) or mouse (E) tumor cells expressing ISRE-mCherry reporter, treated with different doses of CBL0137 for 48 hours. Poly(I:C) - polyinosinic:polycytidylic acid was used as a positive control for reporter activation at 50μg/ml.

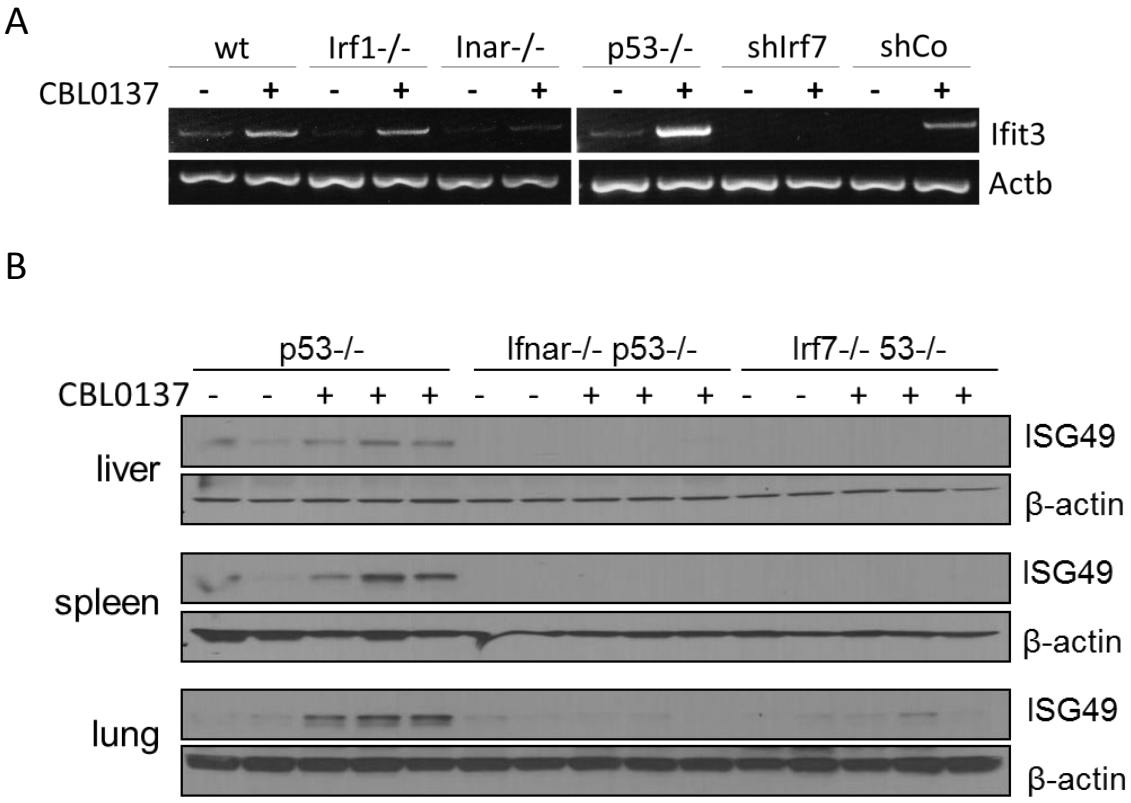

Figure 5. Induction of IFN responsive gene by CBL0137 depends on IFN signaling. A. RT-PCR of RNA from MEF cells of different genotype or wild type MEF transduced with control shRNA or shRNA to Irf7 and treated for 24 hours with 0.5μM of CBL0137. B. Immunoblotting of tissues lysates from mice of different genotypes treated with vehicle control (n=2 for each genotype) or 60mg/kg of CBL0137 (n=3) 24 hours before tissue collection.

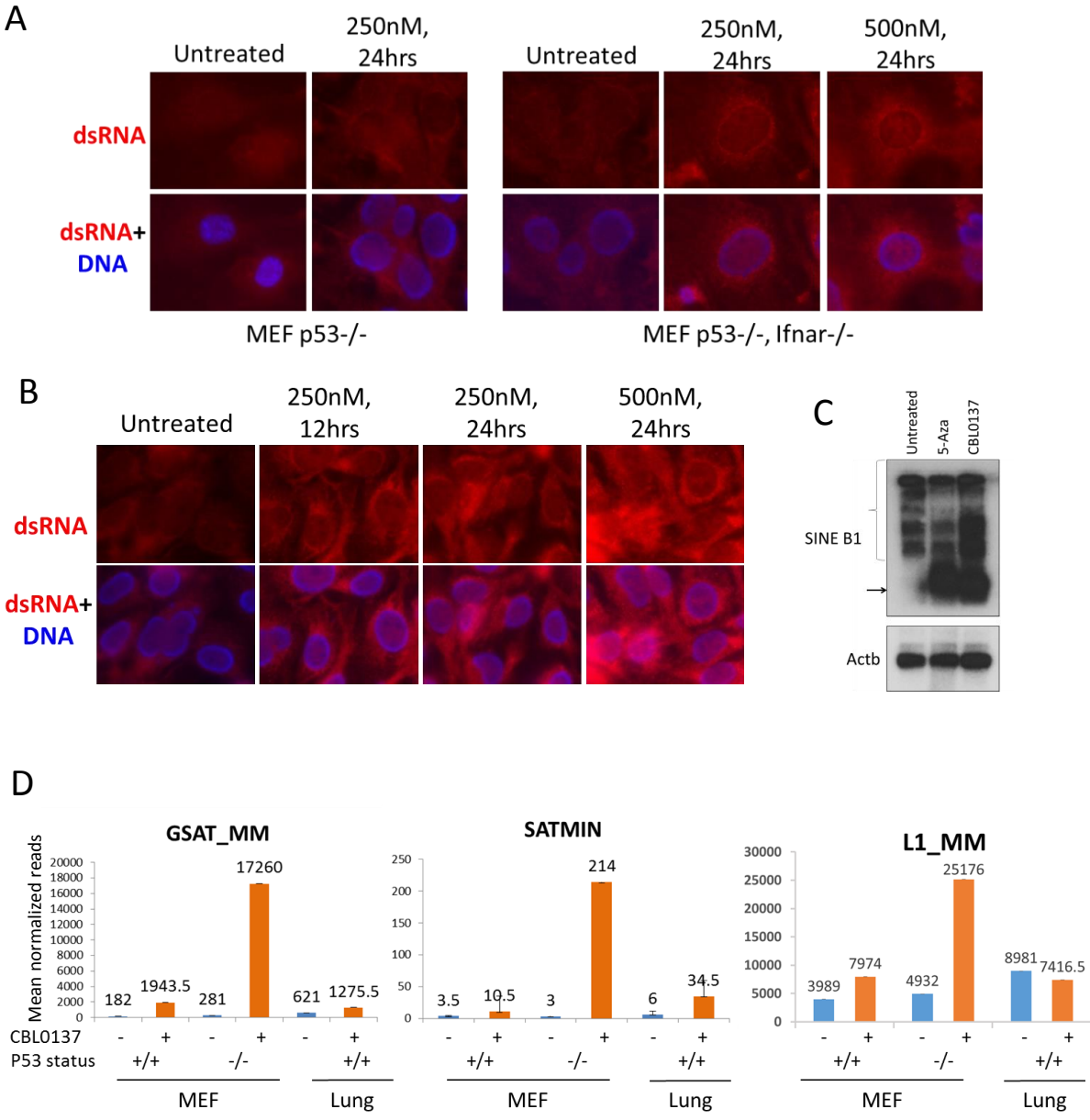

Figure 6. Elevated presence of double stranded RNA in cells and tissues of mice treated with CBL0137. A. Immunofluorescent staining of mouse (A) and human (B) HT1080 cells with antibody to dsRNA (red) and Hoeschst (bluse). C. Northern blotting of RNA from MEF (p53-/-) treated with either 5-Aza for 72 hours or CBL0137 for 48 hours and hybridized with B1 or beta-actin probes. D. Increase in transcripts corresponding to major (GSAT) or minor (SATMIN) satellites or LINE1 in MEF cells or lung tissue of mice treated with either 1μM or 60mg/kg of CBL0137 for 24 hours.

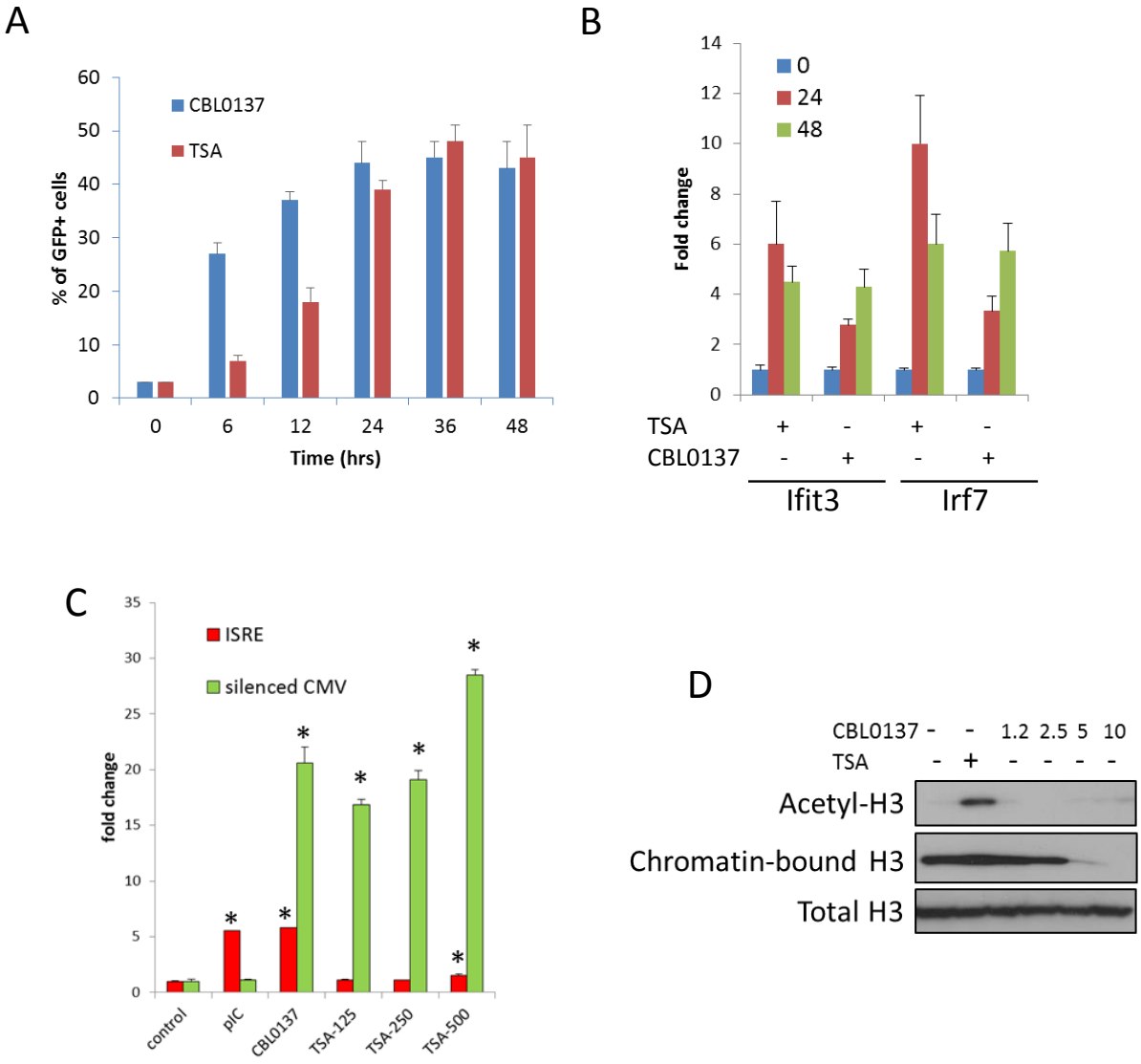

Figure 7. CBL0137 treatment leads to TRAIN by due to chromatin opening. A. Increase in the proportion of cells expressing GFP from silenced CMV promoter in Hela cells treated with either TSA (250nM) or CBL0137 (500nM). B. Changes in the abundance of Ifit3 and Irf7 mRNAs in MEF treated with 500nm of TSA or CBL0137 for 24 or 48 hrs. Quantitation of RT-PCR, mean of two experiments +/- SDV. All changes are significant versus untreated control ($p<0.05$). C. Change in the of the proportion of Hela-TI-ISRE-mCherry cells positive for mCherry and GFP after 48 hours treatment with the indicated agents. TSA concentrations in nM. Mean of two replicates +/-SDV. * - $p<0.05$ vs untreated control. D. Immunoblotting of extracts of Hela cells treated with TSA (200nM) or different doses of CBL0137 (μM) for 24 hours. Acetyl H3 and total H3 was detected in total nuclear extracts, chromatin bound H3 - in chromatin pellet, washed from nucleoplasm with 450mM NaCl buffer.

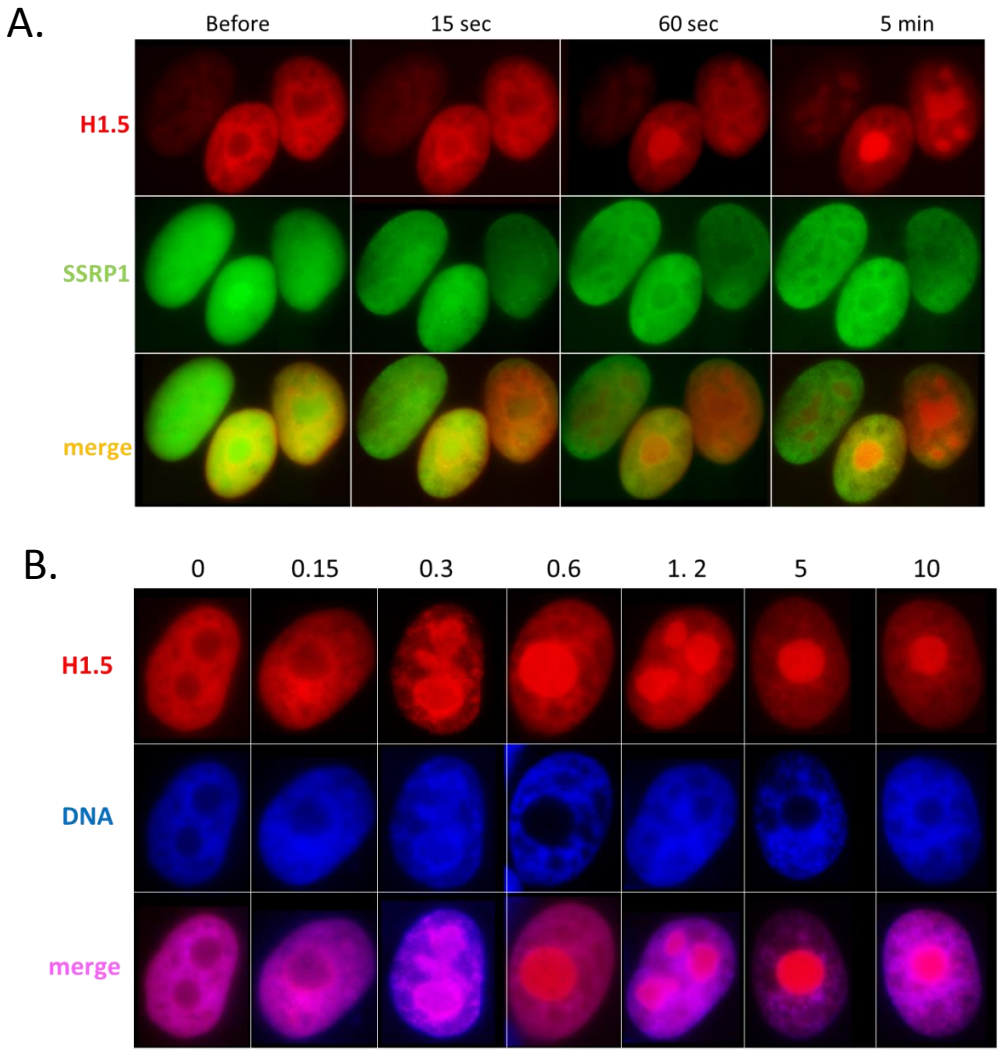

Figure 8. CBL0137 treatment leads to displacement of histone H1. Live cell imaging of HT1080 cells expressing mCherry tagged H1.5 and GFP-tagged SSRP1. A. Images of nuclei of the same cells at different moments after addition of 1μM of CBL0137 to cell culture medium. B. Images of nuclei of cells treated with different concentrations of CBL0137 (μM) for 1 hour.

A

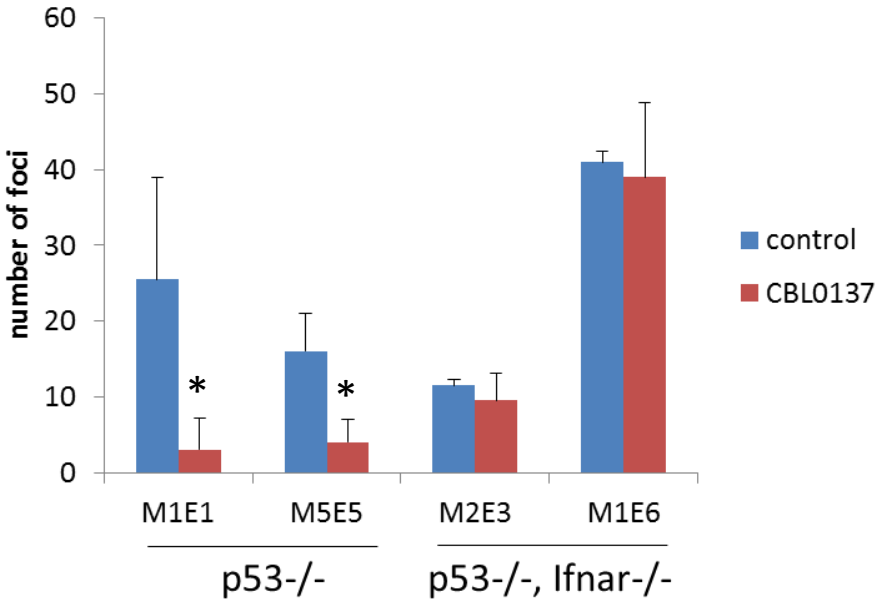

Figure 9. Treatment of cells transduced with H-Rasv12 with CBL0137 leads to the reduction in the number of transformed foci in Ifnar dependent manner. MEF of different background were transduced with lentiviral HrasV12 followed by treatment with 250nM of CBL0137 for 28 hours. Number of foci was detected on day 10 after transduction. Cultures from two embryos of each genotype were used. Mean of two replicates +/-SD. * - $p<0.05$.

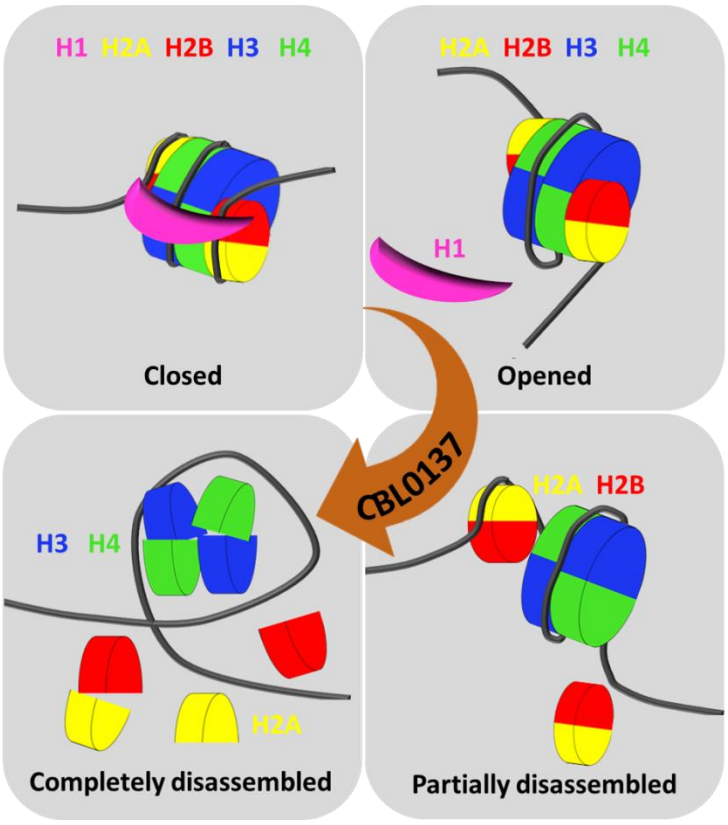

Figure 10. Proposed scheme of nucleosome states in the absence and presence of increasing concentrations of CBL0137.